

# Hebron

## HEBRON PROJECT

Comprehensive Study Report  
Nearshore Bull Arm Spill Trajectory Modelling Report  
February 2011

ExxonMobil



Prepared for:  
Stantec Consulting Ltd.

---

---

**Results from Simulations of Fuel Oil Spills in Bull Arm, Trinity Bay,  
Newfoundland and Labrador**

**ASA Project 2010–261**

**February 2011**

---

---

Prepared by:

**Chris Galagan  
Nicholas Cohn  
Rachel Shmookler**



**Applied Science Associates, Inc.  
55 Village Square Dr  
South Kingstown, RI 02879**

## Executive Summary

ASA has used its SIMAP model system to simulate spills of fuel oil in Bull Arm, Trinity Bay, Newfoundland and Labrador. The model uses wind data obtained from model hindcasts and field measurements, and current data from a hydrodynamic model. The SIMAP model was used in stochastic and deterministic modes to determine the range of possible water surface oiling, oil in water column and shoreline oiling predicted to occur. Spills simulated at this site are instantaneous surface releases of 100 m<sup>3</sup> of marine diesel fuel and 1,000 m<sup>3</sup> of Intermediate Fuel Oil (IFO-180). Simulations were performed for both summer and winter conditions. Winter season spills were simulated with and without sea ice present.

Wind data were obtained from the MSC50 Wind Hindcast model that provides winds for the North Atlantic for the period 1954 through 2008. Wind speed and direction data for the most recent 30 years of this period were used in the oil spill modeling. Wind data collected during a field program run at the Bull Arm site in 1995 through 1997 were used to supplement the model winds and provide wind forcing specific to the oil release location.

Two separate hydrodynamic simulations were carried out using the HYDROMAP model in order to capture the combined tide and wind-driven currents in Bull Arm and Trinity Bay. Tidal current simulations were conducted using 7 astronomical tidal constituents (M2, S2, N2, K2, O1, K1, and P1) to develop tidally-driven surface currents over the entire region. Wind-driven current simulations were conducted for eight wind directions using a constant wind speed of 8 m/s and then added to the tidal current simulation to create a combined current. This results in a current field covering Trinity Bay and Bull Arm that accounts for tide- and wind-driven currents and is used to drive the oil spill simulations.

The stochastic model was used to determine the probability of oil on the water surface, on the shoreline and in the water column exceeding the following thickness and concentration thresholds:

- surface oil average thickness > 0.01 mm (10 µm)
- shoreline oil average thickness > 0.01 mm (10 µm) over the shoreline
- entrained oil (in the water column) average concentration > 10 ppb

Results from the stochastic model simulations are summarized in the table below.

**Summary Table**

Oil Release	Season	Surface Area Oiled at > 0.01mm (km <sup>2</sup> )	Shoreline Oiled at > 0.01mm (km)	Entrained Oil Volume after 30 days (m <sup>3</sup> )
100 m <sup>3</sup> Marine Diesel	Summer	581.4	19.8	58.6
	Winter	371.2	10.1	65.3
1,000 m <sup>3</sup> IFO 180	Summer	1524.8	144.3	0.017
	Winter	1670.5	137.5	0.024

Individual spill events performed as part of the stochastic modeling were ranked to determine the 95<sup>th</sup> percentile spill for oiled sea surface area, oiled shoreline length and entrained oil volume at the defined thresholds. Maps were prepared showing surface oil, shoreline oil and entrained oil for the 95<sup>th</sup> percentile cases. Mass balance graphs depicting the volume of oil present on the surface, evaporated to the atmosphere, entrained in the water column, stranded on the shoreline, and decayed by natural processes are also generated.

# Table of Contents

Executive Summary .....	ii
Table of Contents.....	iv
List of Figures .....	v
List of Tables.....	vi
1. Introduction .....	1
2. Model Inputs and Spill Scenarios.....	1
2.1 Study Area .....	1
2.2 Model Scenarios .....	2
2.3 Oil Characterization.....	3
2.4 Wind Data .....	3
2.5 Current Data .....	6
2.6 Ice Data.....	13
3. Modeling Description .....	16
3.1 Surface Releases of Fuel Oils in Bull Arm .....	16
4. Model Results .....	19
4.1 Stochastic Model Results.....	19
4.2 Deterministic Model Results.....	20
6. References.....	23
Appendix A: SIMAP Model Description.....	1
Appendix B: Stochastic Model Results .....	1
Appendix C: Deterministic Model Results.....	1

## List of Figures

Figure 2.1-1. Map showing the Newfoundland region and spill sites used in the modeling.....	2
Figure 2.4-1. Map of the Bull Arm, Trinity Bay area showing the location of the potential diesel and fuel oil spills and the MSC50 wind data sites.....	4
Figure 2.4-2. Wind rose diagram from the MSC50 model hindcast at location M6012874.....	5
Figure 2.4-3. Wind rose diagram from the Oceans Limited data collected at the Hibernia GBS construction site during 1995 and 1996. ....	5
Figure 2.5-1. Map of the large scale ocean currents in the Newfoundland region. (Source: U.S. Coast Guard, International Ice Patrol). ....	6
Figure 2.5-2. HYDROMAP model grid of Trinity Bay and Bull Arm. ....	8
Figure 2.5-3. Trinity Bay hydrodynamic model grid showing detail in the Bull Arm area. ....	9
Figure 2.5-4. Comparison of observed water elevation (top plot) versus model predicted water elevation (bottom plot) at Long Cove, Trinity Bay. ....	10
Figure 2.5-5. Model predicted mean surface flood tidal currents in the area of Bull Arm. The current vector in the Current Scale window represents a current speed of 1cm/s (0.02 knots). ....	11
Figure 2.5-6. Model predicted mean surface ebb tidal currents in the area of Bull Arm. The current vector in the Current Scale window represents a current speed of 1cm/s (0.02 knots). ....	12
Figure 2.5-7. Model predicted surface currents generated by a west wind in the area of Bull Arm. The current vector in the Current Scale window represents a current speed of 50cm/s (1 knot).....	13
Figure 2.6-1. Total accumulated ice coverage for the period of record from the Canadian Ice Service. ....	14
Figure 2.6-2. Ice concentration chart form the Canadian Ice Service for the week of 12 March, 1990.....	15

## List of Tables

Table 2.2-1. Oil spill scenarios modeled at the Bull Arm location. ....	2
Table 2.3-1. Characteristics of oil used in the spill simulations.....	3
Table 3.1-1. Spills of marine diesel and intermediate fuel oil released at the Bull Arm site modeled using the 3D fates model. ....	18
Table 4.1-1. Summary of surface oiling from the stochastic simulations of marine diesel and intermediate fuel oil released at the Bull Arm site. Values in the table are from the individual spill ranked as the 95 <sup>th</sup> percentile in each category. ....	19
Table 4.2-1. Summary of deterministic model mass balance at the end of the 30-day simulations. ....	21

# **1. Introduction**

ExxonMobil Canada Properties (EMCP) has contracted ASA for oil spill modeling services to simulate spills at locations off the coast of Newfoundland. The SIMAP model was used to simulate spills of fuel oil in Bull Arm, Trinity Bay, and crude oil spills at the Hebron offshore site southeast of St. John's. The model scenarios use wind data obtained from model hindcasts and field measurements, and current data from multiple hydrodynamic models. The SIMAP model was used in stochastic and deterministic modes to determine the range of possible water surface oiling, oil in water column, and shoreline oiling predicted to occur.

This report presents the model input data and model results for simulations of fuel oil spills performed at the Bull Arm site. A companion report provides the same information for spill simulations performed at the Hebron offshore well site. Also included in the current report is a description of the systems used to perform the modeling.

## **2. Model Inputs and Spill Scenarios**

The spill scenarios modeled were defined in consultation with EMCP and ExxonMobil Biomedical Sciences to represent the spills that may occur at the near shore site in Bull Arm. In Bull Arm, the potential spills consist of either marine diesel or Intermediate Fuel Oil (IFO-180) releases from vessels involved in construction of the platform. These spills may occur at any time of year and under a range of environmental conditions, including partial sea ice coverage.

The SIMAP system was used to simulate the fuel oil spills. The model simulates the transport and weathering of the oil released onto the water surface. This section describes the spill scenarios used and the wind, current and ice data defining the environment.

### **2.1 Study Area**

The Island of Newfoundland located in the North Atlantic off the east coast of Canada. The relatively shallow waters of the Continental Shelf extend eastward up to 500 km from the Newfoundland coast. Known as the Grand Banks, this area contains significant petroleum resources. The Hebron field is located near the edge of the Grand Banks, more than 300 km east of St John's (Figure 2.1-1). Bull Arm is a small, relatively deep fjord at the southwest corner of Trinity Bay.

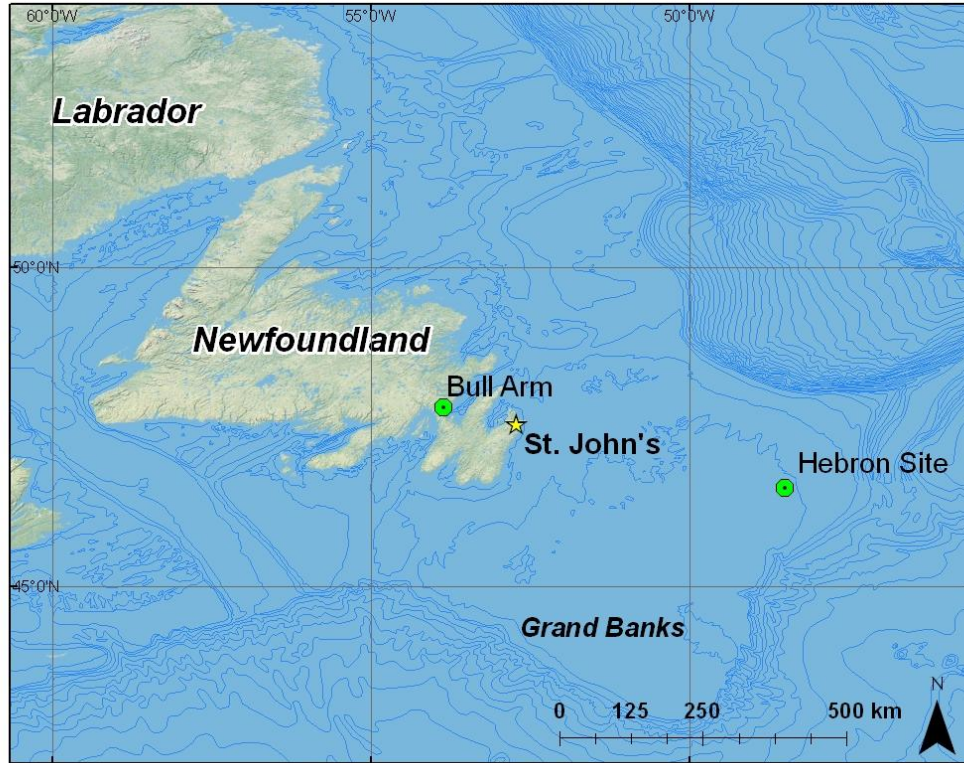


Figure 2.1-1. Map showing the Newfoundland region and spill sites used in the modeling.

## 2.2 Model Scenarios

Multiple spill scenarios were modeled to assess the fate of oil spilled from the nearshore site in Bull Arm. Spills at the Bull Arm site are instantaneous releases of marine diesel fuel and IFO-180 onto the water surface. Each scenario simulates the movement and weathering of the spilled oil for a period of 30 days, a length of time sufficient to allow for all of the weathering processes to occur. Table 2.2-1 displays the specifics for all spill scenarios. The characteristics of the spilled oils are discussed in Section 2.3.

TABLE 2.2-1. OIL SPILL SCENARIOS MODELED AT THE BULL ARM LOCATION.

Scenario	Spill Volume	Spill Duration	Season
<b>Bull Arm (47.818333° N, 53.866667° W)</b>			
Vessel Discharge Marine Diesel	100 m <sup>3</sup>	Instantaneous	Summer
		Instantaneous	Winter - No Ice
		Instantaneous	Winter - 65% Ice
Vessel Discharge IFO 180	1,000 m <sup>3</sup>	Instantaneous	Summer
		Instantaneous	Winter - No Ice
		Instantaneous	Winter - 65% Ice

## 2.3 Oil Characterization

The characteristics of the oil types used in the spill simulations are listed in Table 2.3-1. The SIMAP model uses these characteristics to calculate oil weathering simultaneously with oil transport in the environment.

TABLE 2.3-1. CHARACTERISTICS OF OIL USED IN THE SPILL SIMULATIONS.

Oil	Spill	API Gravity	Density (g/cm <sup>3</sup> )	Viscosity (cP)
Marine Diesel	Vessel in Bull Arm	37.6	0.82910 @ 25° C	4.0 @ 25° C
IFO-180	Vessel in Bull Arm	14.8	0.9670 @ 25° C	2324.0 @ 25° C

## 2.4 Wind Data

Wind data for near shore model simulations were obtained from two sources. One source is the MSC50 Wind Hindcast (Swail et al., 2006), a model reanalysis product that provides hindcast winds for the north Atlantic for the period 1954 through 2008. The data are supplied at evenly spaced points 0.1° apart by Environment Canada, MSC Atlantic Operations. Figure 2.4-1 is a map showing the locations of the MSC50 data nodes in Trinity Bay. The most recent 30 years of the MSC50 wind data were used in the oil spill model simulations. Wind data were also obtained during a field program run at the site of the Hibernia GBS from January 25, 1995, through May 26, 1997, by Oceans Ltd. These data consist of wind speed and direction collected on a 10-minute interval for the 28-month period. These data provide a good picture of how wind inside Bull Arm differs from wind in Trinity Bay.

Figure 2.4-2 is a wind rose showing the distribution of wind directions and speeds at the southern end of Trinity Bay according to the MSC50 model hindcast data obtained for location M12874 (Figure 2.4-1). The wind comes from all directions at this site, but it comes most frequently from the south through the northwest. The wind rose showing the data collected by Oceans Ltd. in Mosquito Cove in 1995-1996 (Figure 2.4-3) shows a predominance of wind coming from the northwest, suggesting that the land bordering Bull Arm is steering the wind along the long axis of the fjord.

The modeling requires a long-term wind record such as the MSC50 model hindcast provides, but the MSC50 data do not include Bull Arm, so it was necessary to correlate the Oceans Ltd. wind data collected in Bull Arm to a nearby MSC50 grid node (M13032) to correct for the difference in wind speed between the two locations and to account for any possible steering affects inside the fjord. From this analysis, a 30-year wind time series specific to the Bull Arm spill site was produced and used in the oil spill model simulations, along with data from the MSC50 sites in Trinity Bay.

Simulations of the fuel oil spills in Bull Arm use a 30-year wind speed and direction time series from the MSC50 model grid nodes in combination with modified wind time series in Bull Arm described above.

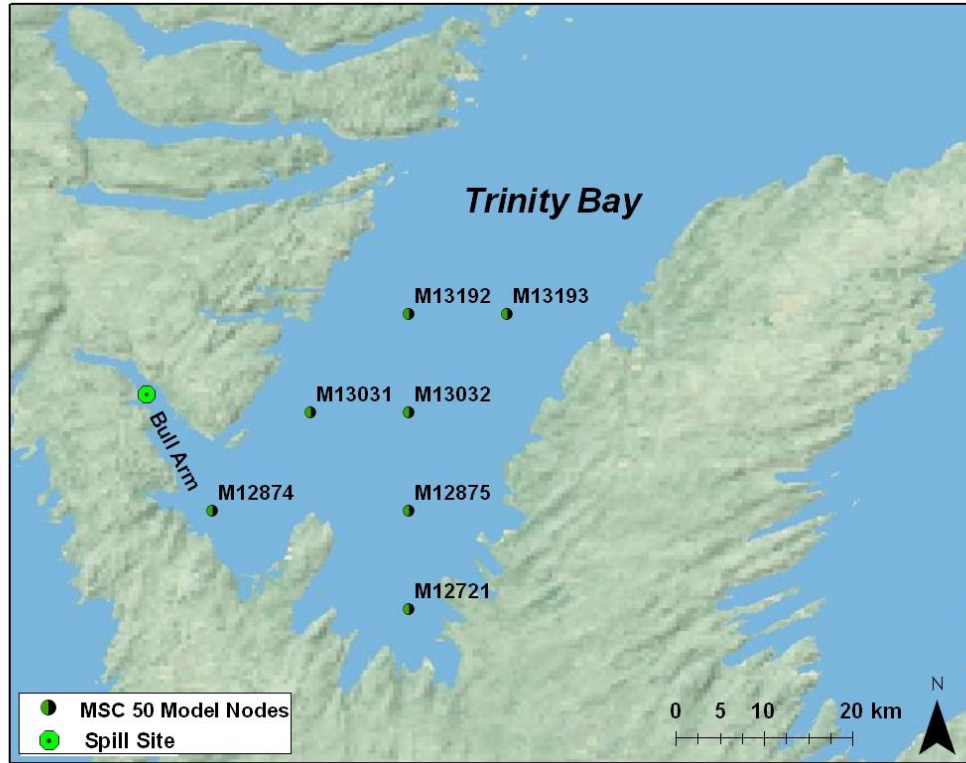


Figure 2.4-1. Map of the Bull Arm, Trinity Bay area showing the location of the potential diesel and fuel oil spills and the MSC50 wind data sites.



## 2.5 Current Data

The Labrador Current dominates the large-scale ocean circulation in the Newfoundland region. This current originates in the Arctic Ocean and flows south along the coasts of Labrador and Newfoundland (see Figure 2.5-1). Currents at smaller scales can be highly variable and it was necessary to develop hydrodynamic model datasets to describe the currents at the Bull Arm and offshore sites sufficient to simulate the movement of spilled oil.

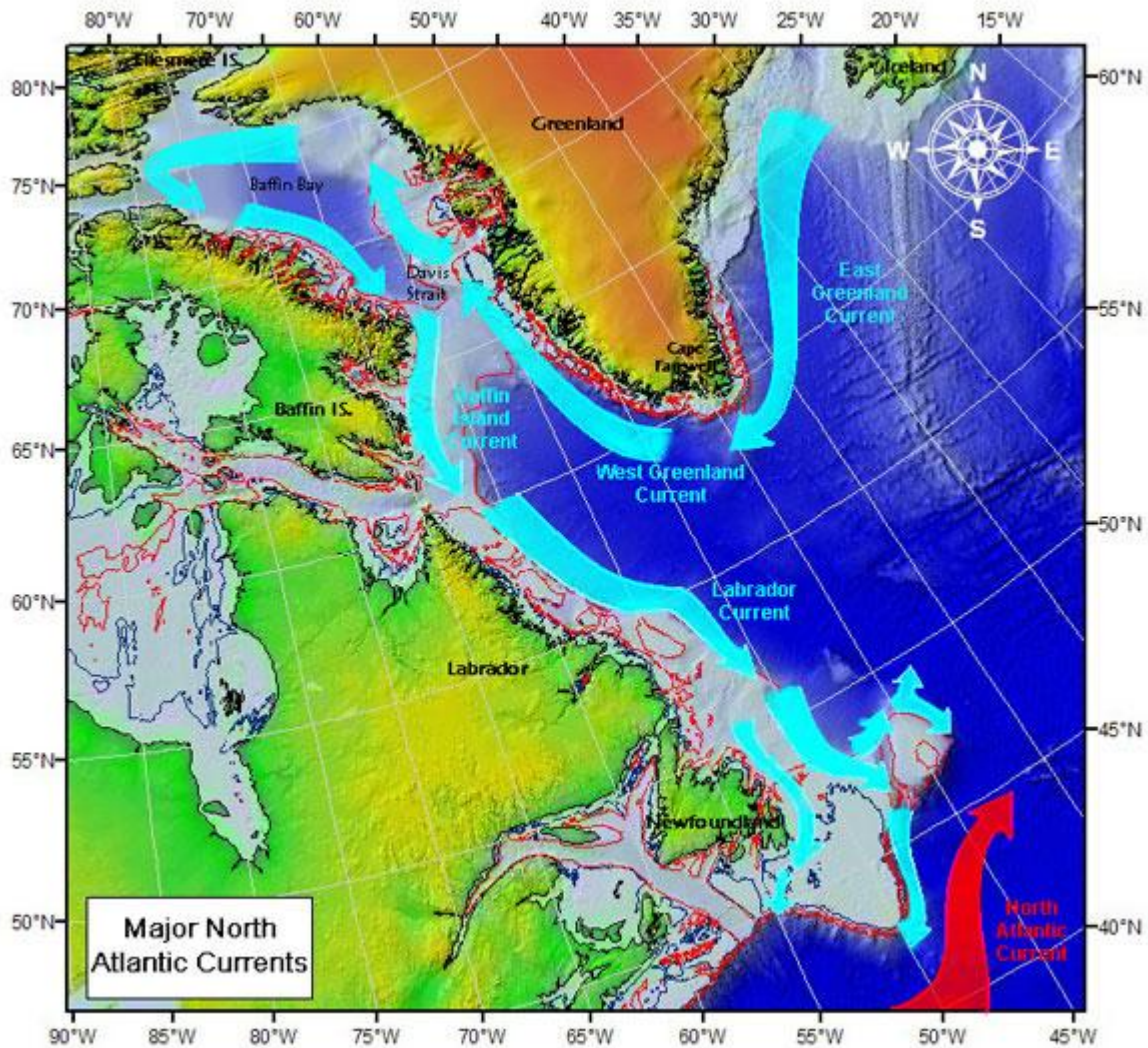


Figure 2.5-1. Map of the large scale ocean currents in the Newfoundland region. (Source: U.S. Coast Guard, International Ice Patrol).

Trinity Bay is an estuary on the northeastern coast of Newfoundland. The long axis of the Bay, approximately 100 km long, is orientated northeast-to-southwest with an opening to the ocean facing the northeast. Bull Arm extends from the southwest corner of the Bay towards the

northwest. Trinity Bay and Bull Arm are relatively deep, hence tidal currents are small and wind driven circulation is a major component of the currents.

A hydrodynamic model grid covering all of Trinity Bay and Bull Arm was prepared with a base cell resolution of 2 km (Figure 2.5-2 shows the grid). The grid cell size gets increasingly smaller moving from the mouth of Trinity Bay to Bull Arm (Figure 2.5-3), to provide maximum resolution in the immediate area of the spill site. Depth data used in the model grid were obtained from navigational charts and the RTM30\_PLUS (Becker and Sandwell, 2008) database.

Two separate hydrodynamic simulations were carried out using the HYDROMAP hydrodynamic model (Isaji et al., 2001) in order to capture the combined tide and wind-driven currents in the area. Tidal current simulations were conducted for 7 astronomical constituents (M2, S2, N2, K2, O1, K1, and P1). The open boundary specification outside Trinity Bay was based on global tide data obtained from the Oregon State University Inverse Tidal Model, TPXO5. TPXO5 is a data assimilation model constrained by satellite altimetry data, TOPEX/Poseidon, as described by Egbert et al. (1994). Using the simulated tide components, it is possible to predict tidal currents within Trinity Bay and Bull Arm for any given date and time. Figure 5.2-4 shows the observed tidal elevation at Long Cove (top plot) and the model predicted tidal elevation (bottom plot) for the same location. The model prediction compares reasonably well with the observed water elevations except that the model lacks small fluctuations seen in the observed data that are a result of wind forcing. Figures 5.2-5 and 5.2-6 are maps of the model-predicted surface currents during mean flood and ebb flow conditions in the vicinity of Bull Arm.

In order to account for the effect of wind on currents in Bull Arm and Trinity bay, wind-driven current simulations were made for eight wind directions with a constant wind speed of 8 m/s. This is done so that a wind-driven current under the range of possible wind directions can be generated and then added to the tidal current simulation to create a combined current. The current generated by each of the eight wind directions represents typical circulation resulting from a day-long wind event. An example surface current resulting from a west wind is shown on the map in Figure 5.2-7.

In the oil spill model, these tide and wind driven currents are automatically reassembled into a single hydrodynamic field. Astronomic tides are constructed based on the date and time of the spill simulation. Based on the average wind speed and direction occurring at this time, one of the eight wind-driven currents is scaled and superimposed on the tidal current. This results in a current field for Trinity Bay and Bull Arm for use in the oil spill model that accounts for tide- and wind-driven currents.



Figure 2.5-2. HYDROMAP model grid of Trinity Bay and Bull Arm.

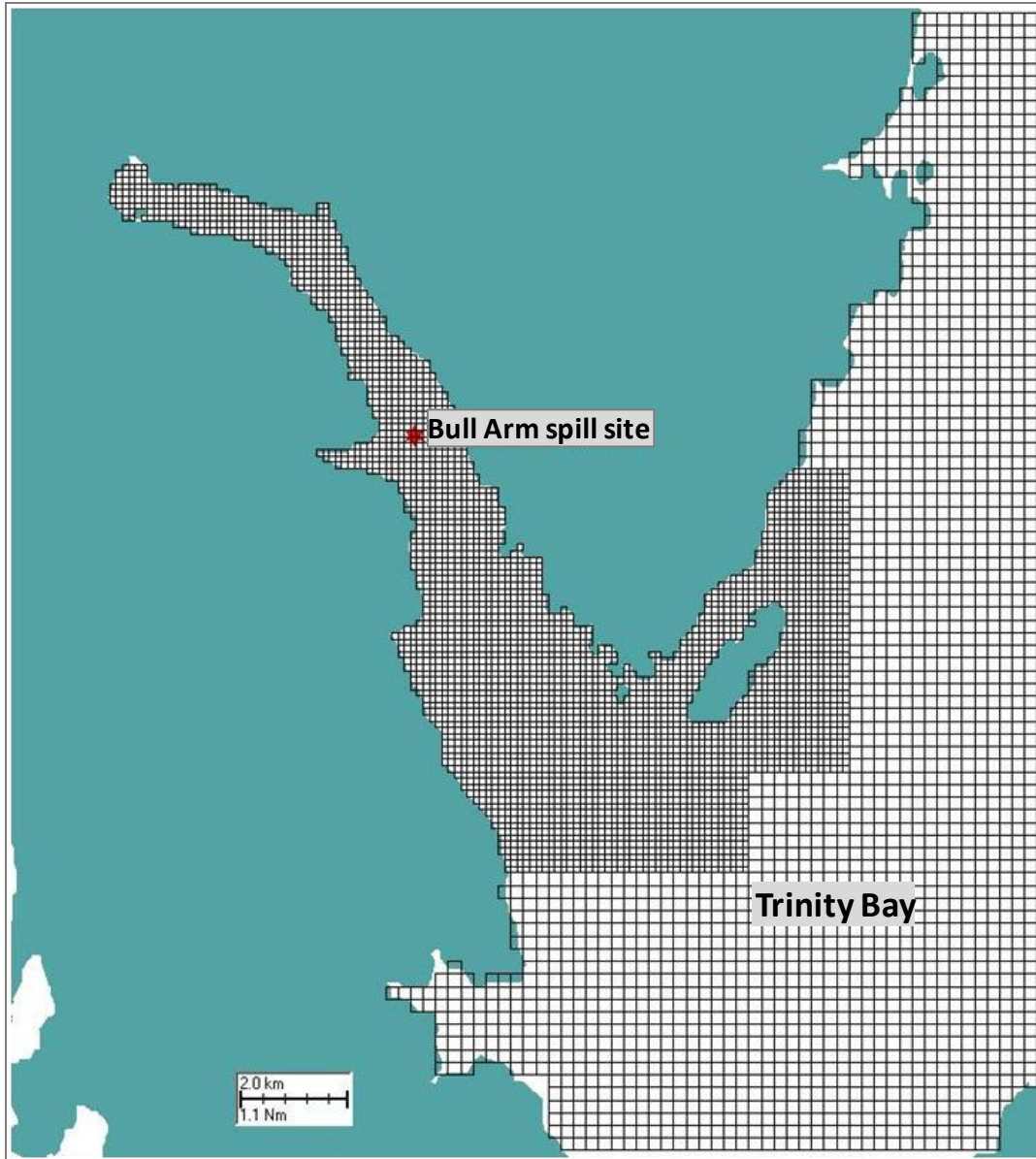
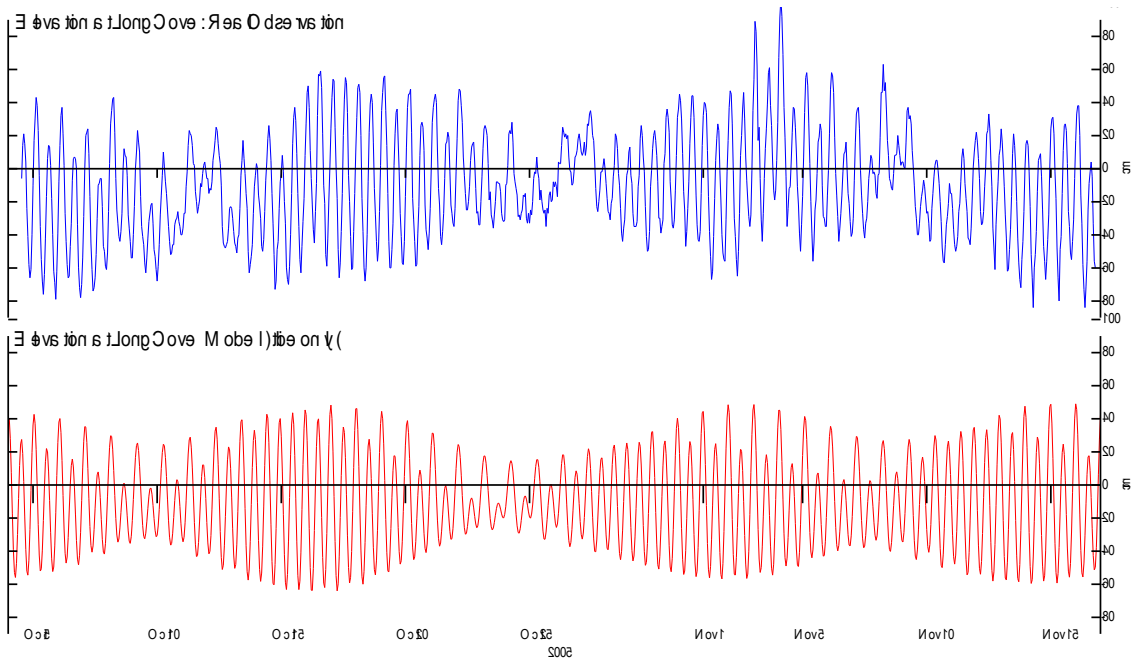


Figure 2.5-3. Trinity Bay hydrodynamic model grid showing detail in the Bull Arm area.



**Figure 2.5-4. Comparison of observed water elevation (top plot) versus model predicted water elevation (bottom plot) at Long Cove, Trinity Bay.**

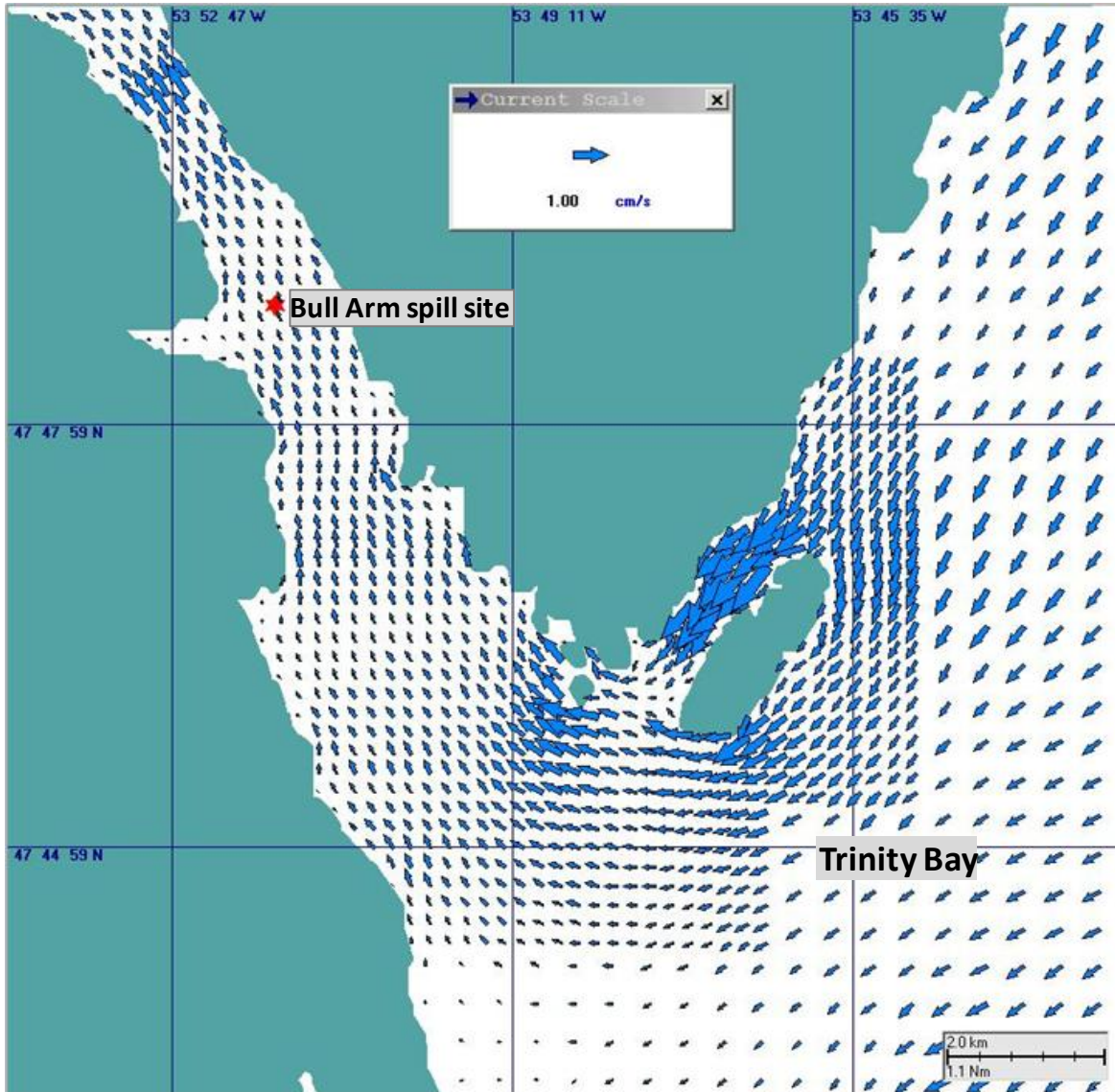


Figure 2.5-5. Model predicted mean surface flood tidal currents in the area of Bull Arm. The current vector in the Current Scale window represents a current speed of 1cm/s (0.02 knots).

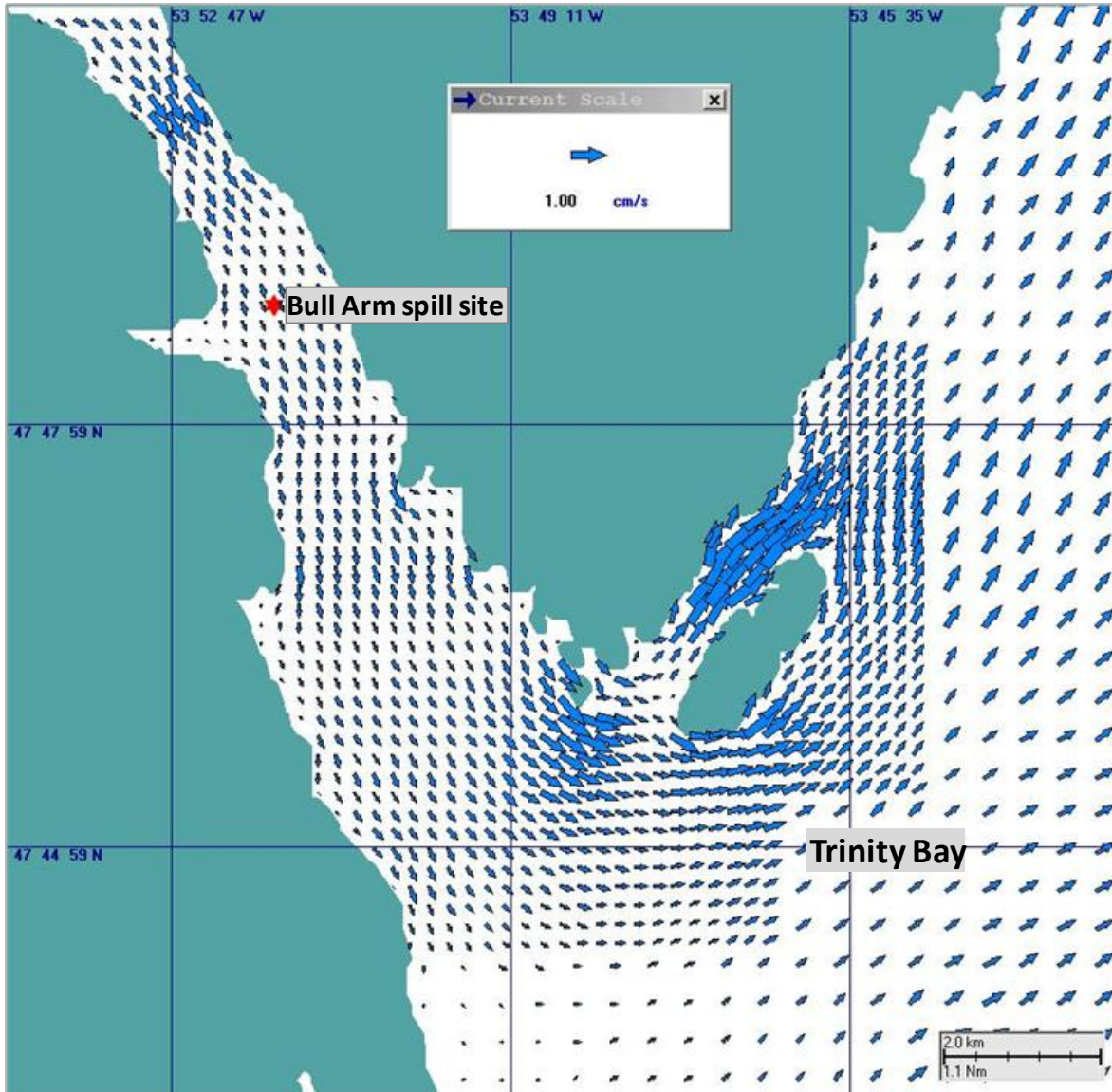
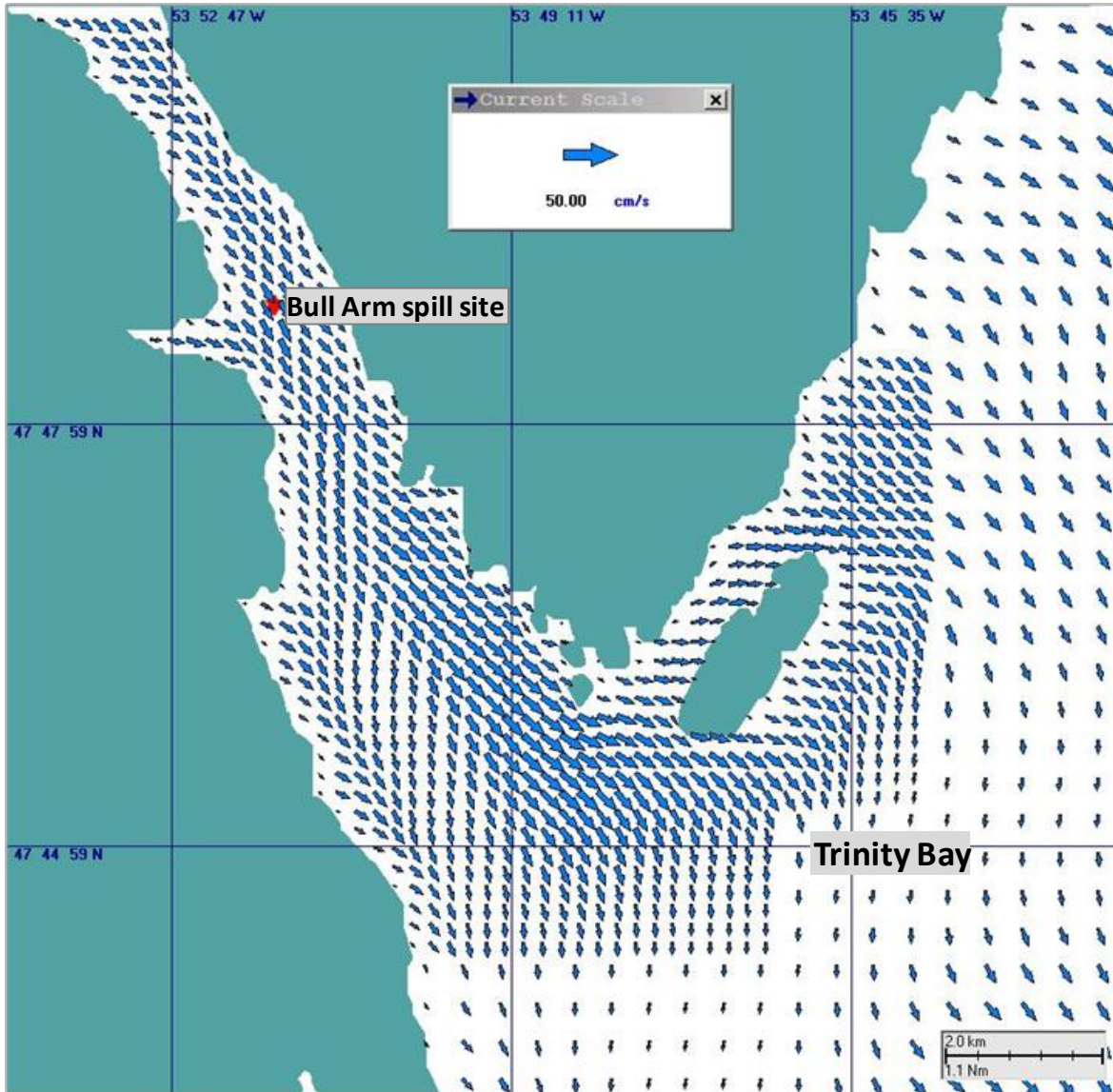


Figure 2.5-6. Model predicted mean surface ebb tidal currents in the area of Bull Arm. The current vector in the Current Scale window represents a current speed of 1cm/s (0.02 knots).



**Figure 2.5-7. Model predicted surface currents generated by a west wind in the area of Bull Arm. The current vector in the Current Scale window represents a current speed of 50cm/s (1 knot).**

## **2.6 Ice Data**

Sea ice is formed in the autumn in the Arctic and sub-Arctic regions of the world. The growth rate of sea ice depends on surface temperature, the depth of snow cover, and the heat flux in the underlying water. The formation and development of sea ice follows a progression of stages, but the exact timing of these stages at any location is not the same from year to year because of subtle differences in climatic conditions. In the Northern Hemisphere during September and October, the air temperature lowers sufficiently to form a thin sheet of ice on the sea. Freezing temperature for average northern ocean salt water of about 3.5 percent salt composition by weight (usually designated 35 parts per thousand) is  $-1.8^{\circ}\text{C}$  ( $28.8^{\circ}\text{F}$ ).

The presence of sea ice in Newfoundland and Labrador waters was below normal during the winter of 2009-2010 (CIS, 2010). The total accumulated ice coverage in east Newfoundland waters set a new record low during last year's winter season. Figure 2.6-1 shows the total accumulated ice coverage offshore the Canadian east coast measured by the Canadian Ice Service since the winter of 1968-69. With the exception of the 2002-2003 ice season, ice coverage over the past 15 years has been below the 40 year average.

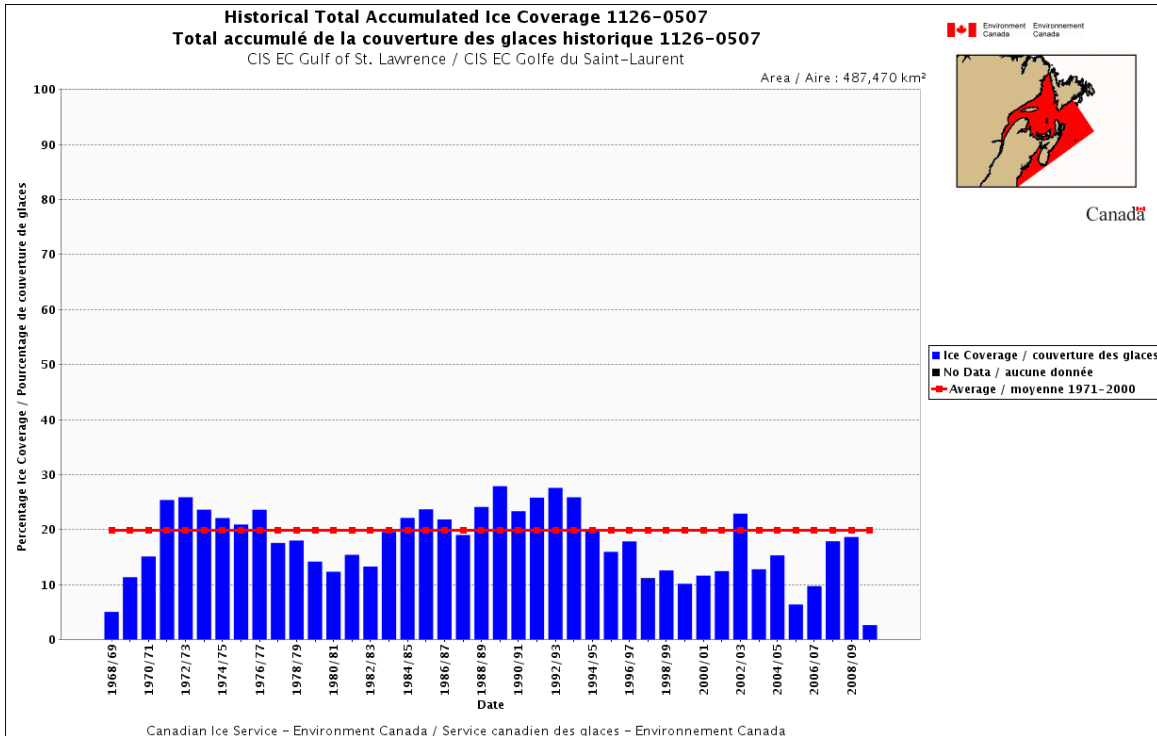


**Figure 2.6-1. Total accumulated ice coverage for the period of record from the Canadian Ice Service.**

Ice coverage in the winter of 1989-1990 was at a maximum extent according to the data collected by the Canadian Ice Service. Figure 2.6-2 shows a map of ice concentration in the Newfoundland region for the week of March 12, 1990. The red areas on the map in Figure 2.6-2 show that 100% ice concentration covers portions of the offshore area east of Newfoundland as well as the southern half of Trinity Bay.

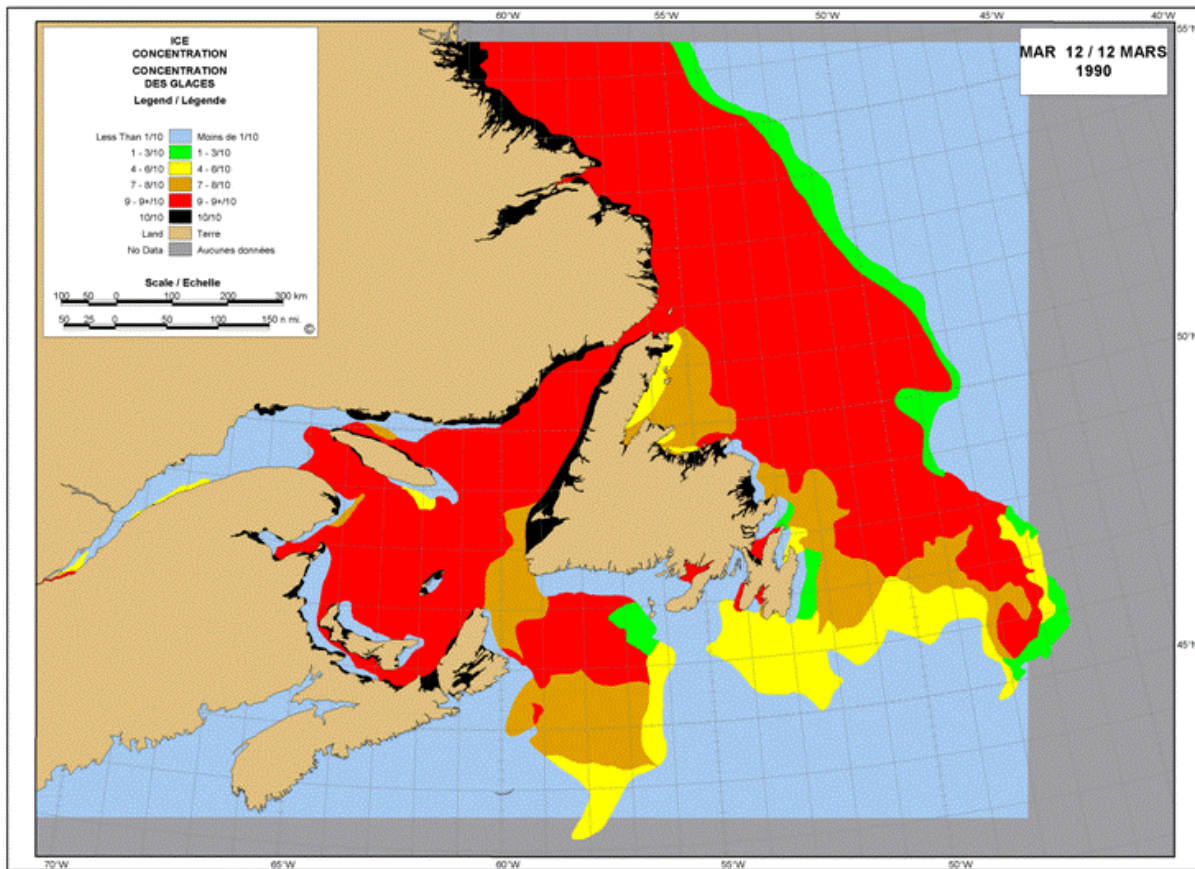


**Figure 2.6-2. Ice concentration chart form the Canadian Ice Service for the week of 12 March, 1990.**

The fate and behavior of spilled oil is greatly affected by the presence of ice. Oil spilled before, during or after freeze-up will follow an arrested pattern of weathering compared to oil spilled on open water. Implementation of algorithms for modeling the movement and fate of oil in the presence of sea ice is based on the percent of ice coverage. From 0 to 30% coverage the ice has no effect on the advection or weathering of a surface oil slick. From 30 to 80% ice coverage, oil advection is steered to the right in the northern hemisphere, surface oil thickness generally increases due to ice-restricted spreading, and evaporation and entrainment are both reduced. Above 80% ice coverage, surface oil moves with the ice, evaporation and entrainment cease and oil thickness, which can vary widely, is calculated as a function of ice thickness. Appendix A contains a brief summary of the algorithms implemented in the SIMAP model for oil spills in sea ice conditions.

Ice coverage in Bull Arm can range from 0 to 100% through the winter season depending on the month and the severity of the winter. Vessel operations during the construction of the Hebron GBS likely will not occur when ice concentration exceeds 65% broken ice coverage. All winter spill scenarios with sea ice present assume that Bull Arm and Trinity Bay are covered with a 65% ice concentration.

### 3. Modeling Description

#### 3.1 Surface Releases of Fuel Oils in Bull Arm

Spills of marine diesel and intermediate fuel oil at the near shore site in Bull Arm were modeled using the SIMAP stochastic and 3D fates models. Instantaneous releases of 100 m<sup>3</sup> of marine diesel and 1,000 m<sup>3</sup> of intermediate fuel oil (IFO-180) at the Bull Arm site were simulated under summer environmental conditions and under winter conditions with and without sea ice present.



**Figure 3.1-1.** Map showing study area with Bull Arm spill site

To determine risks of various resources being oiled, multiple model runs using a range of environmental conditions were evaluated. The Monte Carlo method implemented in the SIMAP stochastic model was used to characterize the potential consequences of spills occurring at the near shore site in summer and winter seasons. For each fuel oil spill scenario the model was run 100 times, with each run using a randomly varied spill date and time so that environmental conditions (currents and winds) were varied within the possible range found in the region.

The stochastic analysis provides two types of information to describe the potential spills: 1) areas that might be oiled and the associated probability of oiling, and 2) for shoreline contact, the shortest time required for oil to reach any location and/or threshold in the areas predicted to be oiled. This information is presented for surface oil (probability only), shoreline oil (probability and time to contact), and subsurface oil (probability only) in maps in Appendix B and in summary tables in subsequent sections of this report. Total hydrocarbons, the group of

chemical that make up crude oil, are divided into two categories, aromatic hydrocarbons, the toxic component of oil, and aliphatic hydrocarbons. For this study only the non-dissolved total hydrocarbons are tracked.

SIMAP's stochastic simulation results provide insight into the probable behavior of potential oil spills under the environmental conditions expected to occur in the study area during each season. The 100 individual model simulations from each stochastic model scenario were ranked to determine the individual spill resulting in the 95<sup>th</sup> percentile for shoreline oiling, water surface oiling and for oil entrained in the water column. For example, the 95<sup>th</sup> percentile spill for surface oiling is the single spill resulting in a surface area oiled at a thickness exceeding a 0.01mm that is greater than or equal to 95% of all spills simulated. The 95<sup>th</sup> percentile spills are identified by selecting the individual spill that ranks as the 95<sup>th</sup> percentile for:

1. Shoreline - shoreline area oiled with an average thickness > 0.01 mm
2. Water surface – surface area oiled by > 0.01 mm thickness
3. Entrained - subsurface oil concentration > 10 ppb remaining at the end of the simulation

The deterministic trajectory and fate simulations using the 3D fates model are performed for the 95<sup>th</sup> percentile simulations identified in each stochastic analysis as defined above. The 18 simulations (three oil threshold criteria times 6 spill scenarios) listed in Table 3.1-1 provide a time history of oil weathering over the duration of the spill, expressed as the volume of spilled oil on the water surface, on the shore, evaporated, entrained in the water column, and decayed.

The spill scenarios listed in Table 3.1-1 list each of the 95<sup>th</sup> percentile spills based on the criteria above for surface, shoreline and entrained oil amounts.

**TABLE 3.1-1. SPILLS OF MARINE DIESEL AND INTERMEDIATE FUEL OIL RELEASED AT THE BULL ARM SITE MODELED USING THE 3D FATES MODEL.**

<b>Oil Release</b>	<b>95<sup>th</sup> Percentile for:</b>	<b>Season</b>	<b>Scenario</b>
100 m <sup>3</sup> Marine Diesel	Sea Surface Oiling	Summer	1
		Winter - No Ice	2
		Winter - 65% Ice	3
	Shoreline Oiling	Summer	4
		Winter - No Ice	5
		Winter - 65% Ice	6
	Subsurface Oiling	Summer	7
		Winter - No Ice	8
		Winter - 65% Ice	9
1,000 m <sup>3</sup> IFO 180	Sea Surface Oiling	Summer	10
		Winter - No Ice	11
		Winter - 65% Ice	12
	Shoreline Oiling	Summer	13
		Winter - No Ice	14
		Winter - 65% Ice	15
	Subsurface Oiling	Summer	16
		Winter - No Ice	17
		Winter - 65% Ice	18

## 4. Model Results

Results of the stochastic modeling are presented first, followed by the 3D fates deterministic model results.

### 4.1 Stochastic Model Results

The stochastic model is used to determine the probability of oiling the water surface, the shoreline and the water column based on specified thickness and concentration thresholds. The thresholds used for the stochastic model simulations in this study are as follows:

- Surface oil average thickness > 0.01 mm (10 µm)
- Shoreline oil average thickness > 0.01 mm (10 µm)
- Subsurface oil (entrained in water) average concentration > 10 ppb

Maps of the stochastic model results are contained in Appendix B. The maps show the predicted probability of oiling; the predicted shoreline contact also shows the minimum time required for oil to reach any place within the oil probability footprint. The summer maps are shown first followed by the winter season results.

#### Summary of Stochastic Model Results

Table 4.1-1 summarizes the results from the Bull Arm stochastic modeling. The table lists the results from the stochastic model simulations for oiled sea surface area, oiled shoreline length and entrained oil volume for the individual spill ranked as the 95<sup>th</sup> percentile. The 95<sup>th</sup> percentile results correspond to the maps of the deterministic model results shown in Appendix C.

**TABLE 4.1-1. SUMMARY OF SURFACE OILING FROM THE STOCHASTIC SIMULATIONS OF MARINE DIESEL AND INTERMEDIATE FUEL OIL RELEASED AT THE BULL ARM SITE. VALUES IN THE TABLE ARE FROM THE INDIVIDUAL SPILL RANKED AS THE 95<sup>TH</sup> PERCENTILE IN EACH CATEGORY.**

Oil Release	Season	Surface Area Oiled at > 0.01mm (km <sup>2</sup> )	Shoreline Oiled at > 0.01mm (km)	Entrained Oil Volume after 30 days (m <sup>3</sup> )
100 m <sup>3</sup> Marine Diesel	Summer	581.4	19.8	58.6
	Winter	371.2	10.1	65.3
1,000 m <sup>3</sup> IFO 180	Summer	1,524.8	144.3	.017
	Winter	1,670.5	137.5	.024

Summer winds are more often from the southwest, which drives oil onto the northeast coast of Bull Arm. Any oil exiting Bull Arm in the summer is driven northeastward up Trinity Bay. Winter winds are most often from the northwest, which moves surface oil out of Bull Arm and onto the

shoreline at the southern end of Trinity Bay and less frequently towards the northeast and the mouth of Trinity Bay.

The smaller volume 100 m<sup>3</sup> marine diesel spills are predicted to have a 10% to 20% probability of leaving Bull Arm during the summer and a 30% to 40% probability of leaving Bull Arm under winter conditions. Spills of 1,000 m<sup>3</sup> of IFO 180 have a 60% to 70% probability of leaving Bull Arm during the summer, and a 70% to 80% probability of entering Trinity Bay during the winter season.

The model predicts that oil from both the marine diesel and IFO 180 spills has a small (<5%) probability of leaving Trinity Bay. Some of the surface oil probability maps in Appendix B show oil exiting the northeast corner of the model grid. This oil is > 10 days old, the volatile components have evaporated, the oil is at the minimum thickness and moving into open ocean.

Marine diesel has a 60% chance of hitting the Bull Arm shoreline in summer, and a predicted 30% probability to do so in the winter season. IFO 180 spills of 1,000 m<sup>3</sup> have a 100% chance of impacting the Bull Arm shoreline in the summer and a 90% chance during the winter season.

Entrained marine diesel oil is predicted to exceed a concentration of 10 ppb 100% of the time within Bull Arm during the summer and winter seasons. Probabilities drop quickly outside of Bull Arm to 10% to 30% during summer and winter seasons for a small area of southwest Trinity Bay. IFO-180 is a highly viscous fuel that shows almost no entrainment into the water column.

## ***4.2 Deterministic Model Results***

Maps of the deterministic model results are contained in Appendix C. Each map in Appendix C depicts the results from one model simulation chosen from the 100 individual simulations completed by the stochastic model. The simulations were selected because they result in the 95<sup>th</sup> percentile for sea surface oiling area, shoreline oiling length or entrained oil volume. It should be kept in mind that each map in Appendix C displays the results from a different individual simulation.

The maps appear in Appendix C in order: surface oil, shoreline oil, and entrained oil. Each map is followed by a mass balance graph depicting the volume of oil present on the surface, evaporated to the atmosphere, entrained in the water column, stranded on the shoreline and decayed by natural processes.

### **Summary of Deterministic Model Results**

Table 4.2-1 lists the mass balance results for all of the deterministic spill scenarios at the end of the 30-day simulation. The table lists oil volumes in cubic meters.

**TABLE 4.2-1. SUMMARY OF DETERMINISTIC MODEL MASS BALANCE AT THE END OF THE 30-DAY SIMULATIONS.**

Oil Release	95 <sup>th</sup> Percentile for:	Season	Surface Oil (m <sup>3</sup> )	Evaporated Oil (m <sup>3</sup> )	Entrained Oil (m <sup>3</sup> )	Oil Ashore (m <sup>3</sup> )	Decayed Oil (m <sup>3</sup> )
100 m <sup>3</sup> Marine Diesel	Sea Surface Oiling	Summer	0	52	19	16	13
		Winter - No Ice	0	13	65	0	22
		Winter - Ice	0	49	0	44	7
	Shoreline Oiling	Summer	0	56	18	14	12
		Winter - No Ice	0	25	46	10	19
		Winter - Ice	0	50	1	42	7
	Subsurface Oiling	Summer	0	18	59	2	21
		Winter - No Ice	0	11	66	1	22
		Winter - Ice	0	51	1	42	6
1,000 m <sup>3</sup> IFO 180	Sea Surface Oiling	Summer*	30	170	0	420	220
		Winter - No Ice*	20	160	0	510	210
		Winter - Ice	0	160	25	655	160
	Shoreline Oiling	Summer	0	170	0	610	220
		Winter - No Ice*	0	160	0	610	220
		Winter - Ice	0	180	20	675	125
	Subsurface Oiling	Summer*	0	155	0	475	200
		Winter - No Ice	25	155	0	570	210
		Winter - Ice	80	170	10	570	170

Spills of 100 m<sup>3</sup> of marine diesel representing the 95<sup>th</sup> percentile for surface oiling are predicted to remain entirely within Trinity Bay during the winter and to result in small amounts of weathered oil leaving the bay during summer. In the winter season, approximately 12% of the oil is predicted to evaporate by the end of the 30-day simulation; more than 50% of the diesel fuel is predicted to evaporate in the summer season spill. The difference in evaporation is due to higher winter wind speeds, which entrain more oil in the water column, making it unavailable for evaporation.

Spills of 100 m<sup>3</sup> of marine diesel representing the 95<sup>th</sup> percentile for shoreline oiling are predicted to impact much of the Bull Arm shoreline and isolated segments of the Trinity Bay shoreline in both the summer and winter seasons.

Spills of 100 m<sup>3</sup> of marine diesel representing the 95<sup>th</sup> percentile for entrained oil are predicted to exceed the 10 ppb concentration threshold for all of Bull Arm and for an area of southwest Trinity Bay in both the summer and winter seasons.

The presence of 65% ice cover reduces the sea surface area covered by marine diesel oil but results in more widespread shoreline impacts. Ice cover significantly reduces the area predicted to exceed the entrained oil concentration of 10 ppb.

Spills of 1,000 m<sup>3</sup> of IFO-180 representing the 95<sup>th</sup> percentile for surface oiling are predicted to oil Bull Arm and extend the length of Trinity Bay during the summer and winter seasons. Approximately 16% of the IFO-180 is predicted to evaporate by the end of the 30-day simulation during both the summer and winter seasons. The IFO-180 is highly viscous, which limits its entrainment and enhances conditions for evaporation.

Spills of 1,000 m<sup>3</sup> of IFO-180 representing the 95<sup>th</sup> percentile for shoreline oiling are predicted to impact much of the Bull Arm shoreline and segments of the Trinity Bay shoreline in both the summer and winter seasons. The summer shoreline oiling is restricted to the east and west shorelines in the southern half of Trinity Bay. Winter season shoreline oiling is predicted to affect primarily the east coast of Trinity Bay.

Spills of 1,000 m<sup>3</sup> of IFO-180 representing the 95<sup>th</sup> percentile for entrained oil are predicted to exceed the 10 ppb concentration threshold for small areas of Bull Arm close to the release site. The IFO-180 is highly viscous and does not readily entrain.

The presence of 65% ice cover reduces the sea surface area covered by IFO-180 and does not significantly change shoreline impacts compared with the no-ice condition. The presence of 65% ice cover is predicted to eliminate any entrained oil concentrations greater than 10 ppb.

## 6. References

- ASCE Task Committee on Modeling Oil Spills, 1996. State-of-the-art Review of modeling Transport and fate of oil spills. *Journal of Hydraulic Engineering* 122(11): 594-609.
- Becker, J. and D.T. Sandwell, 2008. "SRTM30\_PLUS: Data fusion of SRTM land topography with measured and estimated seafloor topography", SRTM30\_PLUS V4.0 May 20, 2008.
- Boyer, T., S. Levitus, H. Garcia, R. A. Locarnini, C. Stephens and J. Antonov, 2004. Objective Analyses of Annual, Seasonal, and Monthly Temperature and Salinity for the World Ocean on a ¼ E Grid, Submitted to *International Journal of Climatology* April 16, 2004, Ocean Climate Laboratory, National Oceanographic Data Center, Silver Spring, MD.
- Bishnoi, P.R. and Mainik B.B., 1979. Laboratory study of behaviour of oil and gas particles in salt water, relating to deepwater blow-outs. *Spill Technology Newsletter* 4(1): 24-36.
- Bishnoi, P.R., A.K. Gupta, P. Englezos and N. Kalogerakis, 1989. Multiphase equilibrium flash calculations for systems containing gas hydrates. *Fluid Phase Equilibria* 53: 97-104.
- Bleck, R., 1998. Ocean modeling in isopycnic coordinates. Chapter 18 in *Ocean Modeling and Parameterization*, E. P. Chassignet and J. Verron (eds.), NATO Science Series C: Mathematical and Physical Sciences, Vol. 516, Kluwer Academic Publishers, 4223-448.
- Bleck, R., 2002. An oceanic general circulation model framed in hybrid isopycnic-Cartesian coordinates. *Ocean Modeling* 4: 55-88.
- Boyer, T., S. Levitus, H. Garcia, R. A. Locarnini, C. Stephens and J. Antonov, 2004. Objective Analyses of Annual, Seasonal, and Monthly Temperature and Salinity for the World Ocean on a ¼ E Grid, Submitted to *International Journal of Climatology* April 16, 2004, Ocean Climate Laboratory, National Oceanographic Data Center, Silver Spring, Maryland.
- Canadian Ice Service, 2010. Seasonal Summary for Eastern Canada, Winter 2009-2010. Produced by the Canadian Ice Service, July, 2010.
- Chassignet, E.P., L.T. Smith, R. Bleck and F.O. Bryan, 1996. A model comparison: numerical simulations of the North and Equatorial Atlantic oceanic circulation in depth and isopycnic coordinates. *Journal of Physical Oceanography* 26: 1849-1867.
- Egbert, G.D., A.F. Bennett and M.G.G. Foreman, 1994. TOPEX/POSEIDON tides estimated using a global inverse model, *Journal of Geophysical Research* 99: 24821-24852.
- Environmental Technology Centre, Environment Canada, 2004. Spills Technology Databases. Oil Properties database. <http://www.etc-cte.ec.gc.ca/databases/OilProperties/Default.aspx>
- French, D., M. Reed, K. Jayko, S. Feng, H. Rines, S. Pavignano, T. Isaji, S. Puckett, A. Keller, F.W. French, III, D. Gifford, J. McCue, G. Brown, E. MacDonald, J. Quirk, S. Natzke, R. Bishop, M. Welsh, M. Phillips and B.S. Ingram, 1996a. The CERCLA type A natural resource damage assessment model for coastal and marine environments (NRDAM/CME), Technical Documentation, Vol. I - Model Description. Final Report, submitted to the Office of Environmental Policy and Compliance, U.S. Dept. of the Interior, Washington, DC, April, 1996, Contract No. 14-0001-91-C-11.

- French, D., M. Reed, S. Feng and S. Pavignano, 1996b. The CERCLA type A natural resource damage assessment model for coastal and marine environments (NRDAM/CME), Technical Documentation, Vol. III - Chemical and Environmental Databases. Final Report, Submitted to the Office of Environmental Policy and Compliance, U.S. Dept. of the Interior, Washington, DC, April, 1996, Contract No. 14-01-0001-91-C-11.
- Gundlach, E.R., 1987. Oil Holding Capacities and Removal Coefficients for Different Shoreline Types to Computer Simulate Spills in Coastal Waters, In Proceedings of the 1987 Oil Spill conference, pp. 451-457.
- Halliwell, G. R., Jr., 1997. Simulation of decadal/interdecadal variability the North Atlantic driven by the anomalous wind field. Proceedings, Seventh Conference on Climate Variations, Long Beach, CA, pp. 97-102.
- Halliwell, G. R., Jr., 1998. Simulation of North Atlantic decadal/multi-decadal winter SST anomalies driven by basin-scale atmospheric circulation anomalies. *Journal of Physical Oceanography* 28: 5-21.
- Halliwell, G. R., Jr., R. Bleck and E. Chassignet, 1998. Atlantic Ocean simulations performed using a new hybrid-coordinate ocean model. EOS, Fall 1998 AGU Meeting.
- Halliwell, G.R, Jr., R. Bleck, E.P. Chassignet and L. Smith, 2000. mixed layer model validation in Atlantic Ocean simulations using the Hybrid Coordinate Ocean Model (HYCOM). EOS, 80, OS304.
- Hu, D., 1996. On the Sensitivity of Thermocline Depth and Meridional Heat Transport to Vertical Diffusivity in OGCMs. *Journal of Physical Oceanography* 26: 1480-1494.
- IOC, IHO and BODC (GEBCO) 2003. Centenary Edition of the GEBCO Digital Atlas, published on behalf of the Intergovernmental Oceanographic Commission (IOC) and the International Hydrographic Organization (IHO) as part of the General Bathymetric Chart of the Oceans; British Oceanographic Data Centre (BODC), Liverpool.
- Isaji T., E. Howlett, C. Dalton and E. Anderson, 2001. "Stepwise -Continuous-Variable-Rectangular Grid Hydrodynamics Model", in Proceedings of the Twenty-fourth Arctic and Marine Oil Spill Program (AMOP) Technical Seminar, Edmonton, AB, pp. 597-610, June 12, 2001
- Kullenberg, G. (ed.), 1982. Pollutant Transfer and Transport in the Sea: Volume I. CRC Press, Boca Raton, FL, 227 pp.
- Lefebvre, A.H., 1989. Atomization and Sprays, Hemisphere Publishing Corp., New York.
- Marsh, R., M.J. Roberts, R.A. Wood and A.L. New, 1996. An intercomparison of a Bryan-Cox-type ocean model and an isopycnic ocean model, part II: The subtropical gyre and meridional heat transport. *Journal of Physical Oceanography* 26: 1528-1551.
- McAuliffe, C.D., 1987. Organism exposure to volatile/soluble hydrocarbons from crude oil spills – a field and laboratory comparison. Proceedings of the 1987 Oil Spill Conference, API, pp. 275-288.
- McDougall, T.J., 1978. Bubble plumes in stratified environments, *Journal of Fluid Mechanics* 85(4): 655-672.
- Nafaa, M.G. and O.E. Frihy, 1993. Beach and Nearshore Features Along the Dissipative Coastline of the Nile Delta, Egypt. *Journal of Coastal Research* 9(2, Spring): 423-433

- National Research Council (NRC), 1985. Oil in the Sea: Inputs, Fates and Effects. National Academy Press, Washington, DC, 601 pp.
- New, A. and R. Bleck, 1995. An isopycnic model of the North Atlantic, Part II: Interdecadal variability of the subtropical gyre. *Journal of Physical Oceanography* 25: 2700-2714.
- New, A., R. Bleck, Y. Jia, R. Marsh, M. Huddleston and S. Barnard, 1995. An isopycnic model of the North Atlantic, Part I: model experiments. *Journal of Physical Oceanography* 25: 2667-2699.
- Okubo, A., 1971. Oceanic diffusion diagrams. *Deep-Sea Research* 8: 789-802.
- Okubo, A. and R.V. Ozmidov, 1970. Empirical dependence of the coefficient of horizontal turbulent diffusion in the ocean on the scale of the phenomenon in question. *Atmospheric and Oceanic Physics* 6(5): 534-536.
- Roberts, M.J., R. Marsh, A. L. New and R.A. Wood, 1996. An intercomparison of a Bryan-Cox-type ocean model and an isopycnic ocean model, part I: The subpolar gyre and high latitude processes. *Journal of Physical Oceanography* 26: 1495-1527.
- Rye, H., O. Johansen and H. Kolderup, 1998. Drop size formation from deep water blow-outs.' SINTEF Report.
- Statoil Memo, 2010. " El Dabaa Field – Monthly metocean data", Martin Mathiesen, Polytec Foundation, 9 July 2010.
- Swail, V.R., V.J. Cardone, M. Ferguson, D.J. Gummer, E.L. Harris, E.A. Orelup and A.T. Cox, 2006. The MSC50 Wind and Wave Hindcast Reanalysis, Ninth International Workshop on Wave Hindcasting and Forecasting, September 25-29, 2006. Victoria, BC.
- VLIZ, 2009. Maritime Boundaries Geodatabase, version 5. Available online at <http://www.vliz.be/vmcdcddata/marbound>. Consulted on 2010-10.